



HAL
open science

Characterization of surface physico-chemistry and morphology of plasma-sized carbon fiber

D. Gravis, S. Moisan, Fabienne Poncin-Epaillard

► **To cite this version:**

D. Gravis, S. Moisan, Fabienne Poncin-Epaillard. Characterization of surface physico-chemistry and morphology of plasma-sized carbon fiber. *Thin Solid Films*, 2021, 721, pp.138555. 10.1016/j.tsf.2021.138555 . hal-03367321

HAL Id: hal-03367321

<https://hal.science/hal-03367321>

Submitted on 6 Oct 2021

HAL is a multi-disciplinary open access archive for the deposit and dissemination of scientific research documents, whether they are published or not. The documents may come from teaching and research institutions in France or abroad, or from public or private research centers.

L'archive ouverte pluridisciplinaire **HAL**, est destinée au dépôt et à la diffusion de documents scientifiques de niveau recherche, publiés ou non, émanant des établissements d'enseignement et de recherche français ou étrangers, des laboratoires publics ou privés.

Characterization of surface physico-chemistry and morphology of plasma-sized carbon fiber

D. Gravis^{1,2)}, S. Moisan²⁾, F. Poncin-Epaillard¹⁾

1) Le Mans Université – CNRS n°6283, Institut des Molécules et Matériaux du Mans, Avenue Olivier Messiaen, 72085 Le Mans, France

2) IRT Jules Verne, Chemin du Chaffault, 44340 Bouguenais, France

Keywords: carbon fiber; cold plasma; plasma polymerization; plasma-sizing; fiber surface wettability, FTIR spectroscopy.

Abstract

Carbon fiber (CF) surfaces were prepared in order to enhance their cohesion in polymer matrixes for composite applications. Among innovative methods allowing the modification of CF surface, plasma technologies, and more specifically on plasma polymerization is known as an eco-process that allows to size, i.e. to coat the CF strands with organic polymer materials. Depending on plasma parameters and chosen organic precursors, the thin film surface physico-chemistry can be tuned to enhance the plasma-processed CF surface properties. The chemical composition, as well as the effect of thin film thickness, were linked to wettability and surface free energy of the coated CF. Among the different plasma polymers, plasma-poly(acetylene) is characterized with higher deposition rate and was the most efficient for improving the wettability of CF surface. Surface chemistry and thickness appear to be the key parameter of controlling the CF surface wettability.

1. Introduction

Polymer composites gain more interest in the transportation industry thanks to their low densities and good mechanical properties. To address the poor mechanical properties of polymers, composites are prepared by reinforcing the matrixes with several materials such as on carbon-based structures: carbon nanotube (CNT), carbon fiber (CF), graphene, etc. However, carbon-based materials are chemically inert, thus their affinity towards the polymer matrixes is low, *in fine* decreasing the composite properties. This implies that carbon-based materials, especially CF, undergo several surface modification processes to improve their compatibility. First, surface treatments are applied to CF surface in order to functionalize it; such a step of the process modifies the CF surface physico-chemistry and further improves their reactivity. Most common industrial processes are dealing with wet oxidative chemistry on the CF surface [1-3] but lately, new dry phase processes are developed to improve the surface properties [4, 5].

After surface functionalization, thin polymer film is deposited of the CF surface; such process is called sizing. Usually, such polymeric thin film bears similar chemical groups as those incorporated in the composite matrix. Such thin film acts as protective layer towards the environment but also eases the handling of the fragile CF. This type of sizing agent can also act as an intermediate layer to reinforce the interface between the CF and the polymer matrix as described in [5-8]. However, most of the sizing are usually performed by immersing the CF in chemical bath in which polymeric sizing agent is dissolved and after drying wraps the fiber. As for the CF surface oxidation, more eco-friendly sizing methods as polymer chain grafting [9, 10], the whiskerization inducing the growth of inorganic materials on the CF surface [11], physical or chemical vapour (PVD, CVD) deposition of CNT [12] are nowadays developed to

replace wet chemical processes. Among them, plasma polymerization can be applied onto CF surfaces [10, 13, 14].

Plasma-polymerization, specifically at low pressure, is a versatile approach since reducing the starting material consumption and retaining the precursor functionality if the plasma parameters are correctly tuned (for example operating at low discharge or pulsed power) [15, 16]. In addition, plasma polymerization has almost no limitation on the chemical structure of the precursor. Thus, many studies report on the plasma-polymerization of silicon-containing precursors such as hexamethyldisiloxane (HMDSO) [17], oxygen-containing monomers such as acrylic acid [18] and maleic anhydride [18-20], nitrogen-containing monomers as acrylonitrile [21], pyridine [22] and various hydrocarbons like styrene, acetylene and benzene [22]. These studies also report on the chemical properties of the plasma-polymer, as well as on the influence of the plasma-polymer on the cohesion of the sized CFs in different polymeric matrixes and on the mechanical properties of the final composite. The physicochemical properties of the plasma-polymer deposited onto the CF surface must be pointed out, as such properties control and predict the interfacial properties of the sized CF and the cohesion of CF-polymer composite. Therefore, this study aims to carefully characterize such properties of the thin plasma-polymeric layer by measuring contact angles on the plasma-sized carbon fiber and by calculating its surface free energy. This study enlightens how such surface property can be influenced by the plasma parameters and thus by the thin film properties, in order to propose an optimized route of the plasma-polymerization on the CF.

2. Materials and methods

2.1 Materials and sample preparation

Commercial available carbon fiber CF (ex-polyacrylonitrile -PAN- T300, Toray) is composed of 12000 strands and therefore such a material is rough and so rough that AFM pictures cannot be recorded. The roughness qualification could be appreciated thanks to SEM image. It is usually sized, thus the CF was desized before any treatment and characterization. For this purpose, CF was dipped in dichloromethane for 24 hours at room temperature, then rinsed in acetone and alcohol before drying at room temperature during at least 5 min. Sample of ≈ 10 cm was cut for each plasma treatment.

2.2 Plasma surface treatment

The stainless steel plasma reactor chamber is maintained under a low pressure vacuum thanks to a turbomolecular pump (Alcatel ATP-80) coupled with a primary rotary pump. The pressure is measured thanks to a wide range capacitive-penning gauge (Alcatel ACC 1009). Ultimate residual pressure before plasma treatment can be sustained at values between 10^{-3} and 10^{-2} Pa, while the working pressure is maintained at ≈ 1 Pa. The glow discharge is applied thanks to a radio-frequency (RF, 13.56 MHz) impulse, between two parallel electrodes separated by a fixed distance of 12 cm. The Caesar RF (Advanced Energy) plasma generator used for this study allows the dissipation of powers ranging from 5 to 100 W, and is coupled with a RF Navio matchbox (Advanced Energy) to keep the reflected power minimal. The plasma generator also allows to initiate pulsed discharge, with different impulse frequencies (ν) and duty cycles (DC). The plasma chamber is equipped with 2 gas lines, each allowing to finely

tune the gas flow rates thanks to gas flow meters (up to 100 sccm). One of the line is devoted to the injection of liquid organic precursors for plasma-polymerisation.

To ensure good adhesion of the plasma-polymer [21, 23], CF was first treated with pure dioxygen (99.5 %) at a constant flow rate of 10 sccm, under a power of 50 W in continuous wave (CW) mode for 5 min. Liquid organic precursor was then vaporized in the plasma chamber. The gas line opening was controlled and defined by measuring the working pressure inside the chamber during deposition of the plasma-polymer instead of measuring a specific flow rate. Plasma polymerization was run either in CW mode, or in pulsed mode to reduce the fragmentation process and retain the intrinsic chemical structure of the precursor. Typical plasma conditions for pre-treatment and plasma polymerization are reported in Table 1.

Table 1. Plasma parameters for O₂ pre-treatment and plasma-polymerization on the CF

Power (W)	Mode	ν (kHz)	DC (%)	Duration (min)
O ₂ pre-treatment				
50	CW	-	-	5
Plasma-polymerization				
10 - 20	Pulsed	5 - 20	8 - 47	10 - 30

The organic precursors supplied by Sigma-Aldrich, used without any further purification are: gaseous acetylene and liquid HMDSO, acrylic acid (AA) contained in quartz tubes connected to the chamber and vaporized thanks to the low pressure. The used solid maleic anhydride (MA) is filled in the quartz tube heating at 60 °C and vaporized in gas line also heated at 60 C°.

CF sample was held on a homemade substrate-holder: CF was stretched on vertical stainless steel poles under a tension of around 1 N. The steel poles themselves were fixed in an acrylonitrile-butadiene-styrene (ABS) plate to isolate the CF from the plasma chamber. Sample

was thus put under the floating potential. For these experiments, the length of the poles was chosen to place the fiber parallel to the electrodes, and at a distance of 6 cm from both.

2.3 Wettability and surface energy

The physico-chemical properties of the untreated and the plasma-sized CF were characterized by wettability measurements. Single strand of the CF was immersed in sampling probe, respectively polar ethylene glycol (EG) or dispersive hexadecane (HD), thanks to a custom aluminium sample-holder. The dispersive and polar components of the surface tension of both liquids are reported in Table 2.

Table 2. Polar (γ_p) and dispersive surface energies (γ_d) of ethylene glycol and hexadecane

	γ_p (mJ/m ²)	γ_d (mJ/m ²)
EG	19.0	29.3
HD	0	24.7

Transparent spectrophotometry tank was completely filled with the sampling liquid, to ensure a flat surface to avoid the contribution of the liquid meniscus. Single strand was then immersed and its wetting profile was recorded in static mode thanks to the goniometer Krüss G10 DSA100.

The surface free energies were calculated by the Owens-Wendt method [24]. To calculate the contact angles, Young-Laplace equation (eq. 1) was solved for a wetting profile on vertical solid plane as described by Arts *et al.*[25]. In this case, coordinates (x ; y) of the profile were measured on the wetting pictures thanks to the software ImageJ. A typical picture of wetting meniscus of a vertical carbon fiber is shown in Fig. 1a. The (x ; y) coordinates measured here are x , the lateral distance from the wall, in this case one side of the CF, and y , the height of the

profile at the respecting x position. The height of the profile is measured from the planar liquid-air interface ($y = 0$) for which x would be infinite. To solve such an equation, two other data must be taken into account: the capillary rise h at $(x; y) \equiv (0; h)$, and the capillary length l_c , which stands for the distance from the CF at y almost equal to 0: $(x; y) \equiv (l_c; 0)$.

$$\frac{x}{l_c} = \operatorname{arccosh}\left(\frac{2l_c}{y}\right) - \operatorname{arccosh}\left(\frac{2l_c}{h}\right) + \sqrt{4 - \frac{h^2}{l_c^2}} - \sqrt{4 - \frac{y^2}{l_c^2}} \quad (\text{eq 1})$$

Fig. 1b shows good agreement between the fit of the equation (1) and the measured values $(x; y)$. Then, the contact angle (θ) of both liquids is calculated from the following equation (2) and the extracted values of h and l_c issued from the profile curve.

$$\theta = \arcsin\left(1 - \frac{h^2}{2l_c^2}\right) \quad (\text{eq 2})$$

The contact angles of HD and EG then allow to calculate the surface free energy of CF and its respective polar and dispersive components.

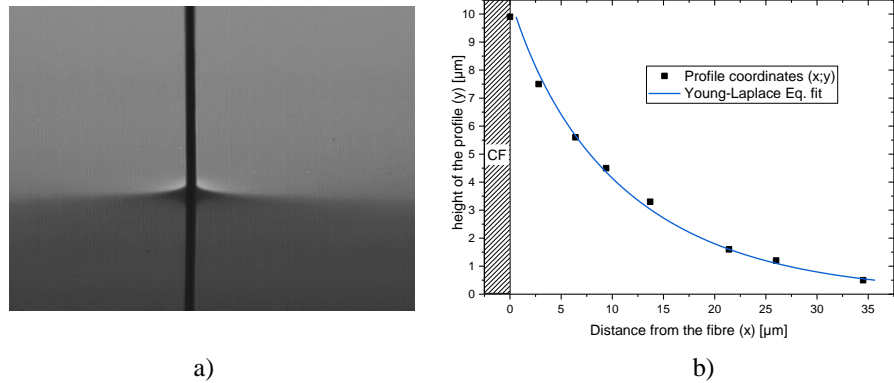


Fig.1. Wetting profile of the pristine ex-PAN T300 CF immersed in hexadecane (a); plotted profile as measured on the picture (dots) and the corresponding Young-Laplace fitting (line) (b). For easier fitting purpose, coordinates axes are swapped right.

2.4 Chemical analysis: Fourier Transform Infrared spectroscopy

Fourier Transform Infrared (FTIR) spectra of the CF itself, layered with the plasma-polymer (pp) and for the pp are recorded on a BRUKER Vertex V70 spectrometer between 400 and 4000 cm^{-1} with DTGS detector, considering 40 scans and 4 cm^{-1} resolution. For transmission analyses, pristine CF was compressed with 150 mg of KBr powder pre-dried for 3 days at 80 °C and the pp thin film coated on KBr pellet was characterized thanks to the transmission mode to gather more resolute spectra of the thin film without the CF contribution; while the FTIR spectra of the CF and the pp deposited on the CF were obtained via the attenuated total reflexion -ATR- mode. Ambient air signature of the environment background was subtracted; for the transmission mode, background and sample spectra were acquired under rough vacuum ($p < 100 \text{ Pa}$) and in ATR mode, spectra are systematically corrected to suppress the dependency of the wavenumber on the analysis depth. Subsequent data analysis included the correction relative to CO_2 and H_2O adsorption on the sample surface, and the polynomial manual correction of the baseline.

2.5 Raman spectroscopy

Raman spectroscopy run on Horiba Xplora Raman spectrometer built on an Olympus BX41 confocal microscope (x100 optical objective) was applied to determine the crystalline of the treated CF. Spectra are recorded with a monochromatic green laser ($\lambda = 532 \text{ nm}$, power = 5 mW), in the range of 500 and 2000 cm^{-1} and the dispersive system consists of a network with 600 strokes/mm. Scan numbers and durations were kept minimal to avoid CF surface destruction, respectively < 10 and $< 40 \text{ s}$.

2.6 Scanning electron microscopy

SEM analyses were run on a JEOL JSM 6510 LV SEM (tungsten filament). As CF is semi-conductor, no specific preparation of the samples was needed to compensate electrostatic charge. However, to avoid degradation of the CF surface, while limiting the surface charging, the analysis was performed with a 35 μm spot size under an acceleration voltage of 10 keV.

2.7 Atomic force microscopy

The thickness of the deposited organosilicon film was determined on Si/SiO₂ wafer by AFM (Bruker Innova). A mask was placed on a part of the substrate before the deposition. Once the deposition was completed, the mask was removed and the top level corresponded to the thickness of the organosilicon film was measured. Area of 50 \times 50 μm^2 of the coated Si/SiO₂ substrate was scanned in tapping mode at ambient air. The film thickness was determined using Gwyddion software.

3. Results and discussion

The following study reports on the plasma deposition of four different plasma-polymers: ppHMDSO, ppAA, ppMA and ppAc; the co-deposition of ppAc-co-MA was also characterized since leading to improved properties [26, 27]. Such a plasma-sizing aims to provide a protective thin film onto the CF surface, as well as a chemically reactive surface in order of enhancing the cohesion between CF and polymeric matrix. These plasma-polymers were chosen because they

can adhere to the CF surface thanks to the formation of covalent bonds at the interface and they provide a surface chemistry increasing the treated CF compatibility with the polymer matrix [2, 4, 5] as well as the impregnation process of liquid matrixes before curing [28]. More specifically, the ppHMDSO composed of SiO_x groups has a strong affinity for epoxy resin matrixes and leads to resilient composites [17, 29-31]. Both acidic ppAA and ppMA enhance the wettability of the polymer matrix and allow the covalent bonding of their surface functions with epoxy groups [30, 32-34]. Moreover, the ppMA should be especially efficient thanks to the high O/C ratio and its anhydride function as observed for different composites [5, 18, 20, 35], even for inert matrixes such as poly(propylene) [18-20]. Finally, the desired objective of the improvement of composite cohesion also requires to take into account of the plasma process itself that must avoid any degradation of the CF during its treatment but also of the deposited matter in order to retain the functionality of the gaseous precursor [15, 16, 30]. Therefore, all the described processes here are run under mild plasma conditions (low discharge power, pulsed plasma with low duty cycle or low impulse frequency).

3.1 Characterization of the carbon fiber after the desizing process

Since the studied material is commercial ex-PAN T300 fiber received as sized fiber, a desizing process was performed as described in the experimental part. Therefore, its efficiency must be verified and the cleaned CF characterized. Raman (Fig. 2a) and FTIR (Fig. 2b) spectroscopies of the desized CFs were performed as quick and reliable methods to characterize the CF surface; assignment of the FTIR vibration bands is reported in Table 3.

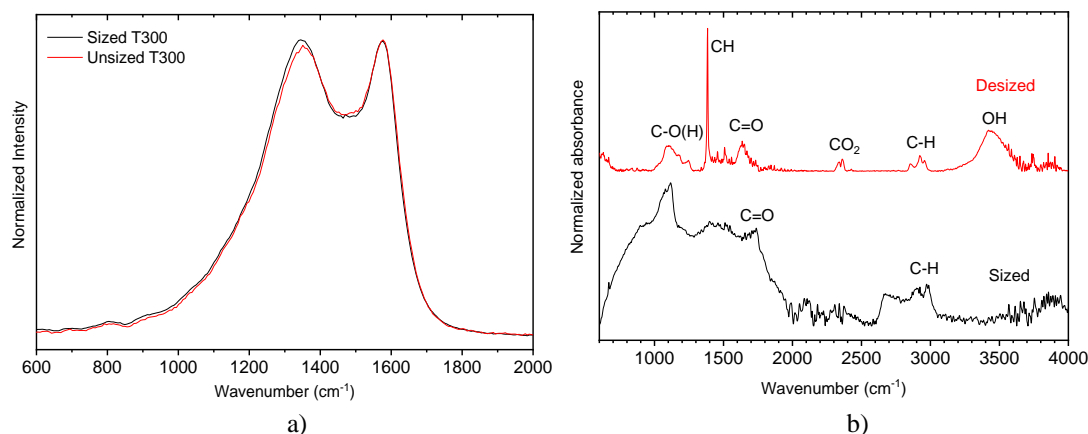


Fig. 2. Raman (a) and FTIR (b) spectra of CF, as-received (sized) and desized CFs with dichloromethane.

Raman spectra (Fig. 2a) are composed of two main bands at 1350 cm^{-1} and 1575 cm^{-1} , so-called respectively the D (disorder) and G (graphitic) bands [36-39]. Each band represents the resonance of the phonons of different crystalline domains: the disorder band is assigned to the amorphous carbon and some contributions of the sp^3 carbon atoms included in C-C bonds; the graphitic band is dependant of the graphitic plane vibrations. Their relative areas give information on the sp^2/sp^3 balance or the ratio between the crystalline and amorphous graphitic domains in the sampled depth. The G band also presents a shift, usually bathochromic over up to 10 cm^{-1} , which indicates the size of the crystalline domains, i.e. if the graphite crystal is monocrystalline or polycrystalline [36-39]. As shown in Fig. 2a, Raman spectra of as-received sized CF and desized CF with dichloromethane are almost similar. The Raman spectrum of the desized CF shows no shift or variation in the area of the G band. This indicates that the chosen sizing does not alter the crystalline structure of the fiber. Therefore, the only small decrease of the intensity of D band noticed with desized CF must be interpreted as a decrease of sp^3 sites rather than a more pronounced crystalline structure [36]. Indeed, these chemical defects can be assigned to the contribution of the added polymeric sizing agent deposited on the CF.

Table 3. Main FTIR vibration bands of the desized CF

Wavenumber (cm ⁻¹)	assignment
500 to 1200	C-H fingerprint
1388	CH bending
1600	C=O and C=C
2350	Adsorbed CO ₂
2700 to 3000	C-H stretching
3400	OH stretching

The FTIR [40-43] spectrum of the sized fiber (Fig. 2b) shows a noisy signal composed of two main features. The first one, the most intense, is ranging from 600 to 1980 cm⁻¹ while the second feature is observed between 2600 to 3045 cm⁻¹. These broad peaks are hardly assigned to any bond vibration. Nevertheless, different vibration modes may be respectively identified at 1120, 1740, 2900 and 2980 cm⁻¹. The first peak at 1120 cm⁻¹ is assigned to the stretching of the C-O bonds more likely belonging to alcohol or ether groups since the vibration mode of C-O of esters appears at higher wavenumbers. The peak at 1740 cm⁻¹ is related to carbonyl groups while the two last bands (2900 and 2980 cm⁻¹) are significant of the presence of aliphatic carbon. The low signal to noise ratio of the spectrum is induced by the lower intensity of the overall signal in terms of that one obtained for desized fiber but it could also be caused by the sizing agent itself. Indeed, commercial sizing agent is in most cases composed of epoxy resin. So, the observed FTIR spectra in Fig. 2b should correspond to a hybrid spectrum of the sizing agent blended with the pristine CF signal, the latter being described as follows. The FTIR spectrum of the desized CF (Fig. 2b, Table 3) is composed of an intense band at 1380 cm⁻¹ and another one less intense between 2700 and 3000 cm⁻¹, assigned respectively to the bending and the stretching vibration of C-H of -CH₃ groups. The broad band centred around 1600 cm⁻¹ corresponds to carbonyl (C=O) and carbon double bond (C=C), originated from surface oxidation at the ambient atmosphere. The other broad and less intense bands centred around 2350 cm⁻¹ and 3400 cm⁻¹ correspond to adsorbed CO₂ and humidity [44]. Therefore, the improvement of the signal, as well as the easier assignment of the main bands in the case of the desized CF with no characteristic peaks of any pollutant or sizing agent indicates that the

desizing process allows to efficiently remove the polymeric thin film deposited on commercial available CF.

3.2 Chemical structure of the plasma-deposit and the corresponding interfacial bonding with desized carbon fiber

The deposition of the ppHMDSO, as for also the other precursors is operated in mildest conditions preserving the HMDSO chemical structure [45]. Such deposited layer is characterized by FTIR spectroscopy (Fig. 3, Table 4).

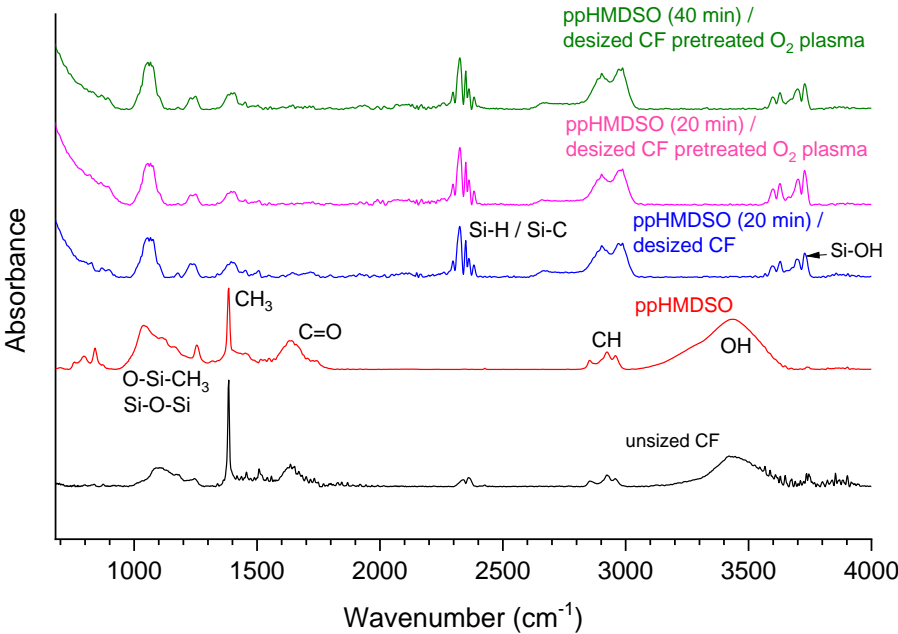


Fig. 3. Influence of the CF preparation (with or without O₂ plasma pre-treatment), of the duration of HMDSO plasma deposition ($p = 2$ Pa, $P = 10$ W, $DC = 8\%$, $\nu = 5$ kHz).

Table 4. Main FTIR bands assignment of the HMDSO plasma-polymer

Wavenumber (cm ⁻¹)	Assignment
ppHMDSO on KBr	
843, 1060 and 1250	Si-O-R
1035	CH ₃ -Si-O or disiloxanes (R ₁ -Si-O-Si-R ₂)
1383	CH ₃ bending

1730	C=O
2350	CO ₂ adsorbed on CF
2700 to 3000	C-H stretching
3400	OH
ppHMDSO on CF	
2150 - 2250	Si-H and Si-C
3600	Si-OH

FTIR spectrum of ppHMDSO deposited on KBr pellet shows most of the characteristic vibration bands of Si-O bonds: Si-O-Si (843, 1250 cm⁻¹), Si-O-CH₃ (1060 cm⁻¹), Si-O-C / disiloxanes (R₁-Si-O-Si-R₂) (1035 cm⁻¹). The organic counterpart of layer composition is confirmed by the presence of the characteristic C-H stretching band from 2700 to 3000 cm⁻¹. Carbonyl groups highlighted by the band centred around 1730 cm⁻¹ indicate surface oxidation of the polymer thin film. The characteristic broad band of hydroxyl groups (-OH, 3400 cm⁻¹) is also observed, probably due to adsorbed ambient water. When the same precursor is deposited onto CF, some FTIR vibration modes are not anymore observed (-OH, 3400 cm⁻¹) while others appear (adsorbed CO₂, 2350 cm⁻¹, between 2150 and 2250, 3600 cm⁻¹). The new bands around 2150 and 2250 cm⁻¹ are significant of Si-H and Si-C bond resonances, while that one at 3600 cm⁻¹ is attributed to silanol compounds. Even if the FTIR analyse does not allow to determine the respective proportions of Si-C and Si-H, the appearance of this band could be explained by the formation of covalent bonds between the plasma deposit and the CF. Nevertheless, if derivate silanes are the major compounds, their formation is only observed in presence of CF since other deposits are done on KBR pellet and they should also reflect the ppHMDSO / CF interface and its influence on the ppHMDSO growth. Same conclusion can be drawn with the appearance of Si-OH bonds. The grafting from the CF may also induce shorter ppHMDSO chains as observed in [36] and therefore with more end-groups that can age in ambient atmosphere. Since interfacial bonds are noticed, the ATR mode appears to be more sensitive than the simple transmission mode with KBr pellet, this could be explained by multiplication of the recorded ATR signal on carbon fiber composed of 12000 strands.

Lastly, it can be noted that the dioxygen plasma pre-treatment of the CF does not induce significant variations in the FTIR spectrum; the same observation can be drawn from the deposition time influence (from 20 to 40 min). In this case, the pre-treatment and a longer deposition does not seem to induce variation in the pp thin film chemistry.

Despite the ATR-FTIR spectroscopy leads to a mean value of the structure of CF bundle (100 μm spot size), as it gives evidence of interfacial covalent bonds, we could assume that the ppHMDSO is deposited over a significant area of the CF. Indeed, SEM micrographs show the homogeneity of the ppHMDSO (Fig. 4).

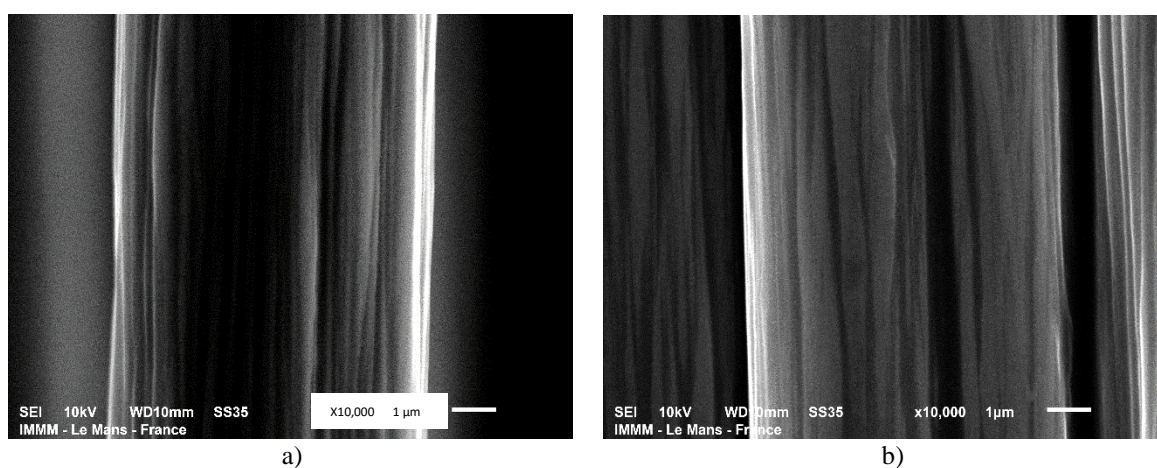


Fig. 4. SEM pictures (x 10,000, 1 μm scale) scale of desized CF (a) and HMDSO plasma-sized- O_2 -plasma-oxidized CF (b) (plasma deposition: $p = 2 \text{ Pa}$, $P = 10 \text{ W}$, $\text{DC} = 8 \%$, $\nu = 5\text{kHz}$).

The desized CF strands (as well as after O_2 plasma pre-treatment, not shown here) present grooves parallel to the fibre axis with variable widths (Fig. 4a). Any particular difference in the surface topography after the HMDSO plasma polymerisation is observed leading to the conclusion that the ppHMDSO deposition should be homogenous overlaying smoothly the cavities of the inherent surface topography of the CF (Fig. 4b). The quite inhomogeneous strand diameter, among every strand of the CF was measured around $6.2 \pm 0.8 \mu\text{m}$ and it does not vary significantly after the plasma deposition, inducing the idea of thin deposited film.

In case of the plasma polymerization of acrylic acid (AA, ppAA), the ppAA FTIR signature is rather simple with only few main characteristic features (Fig. 5, Table 5). Aliphatic carbons are identified by C-H bending and stretching at respectively 1380 and 2900 cm^{-1} . An intense and wide band also appears around 1700 cm^{-1} assigned to carbonyl groups (C=O), showing the carboxylic acid function retention. As noticed with ppHMDSO layered on CF, the FTIR spectra of the ppAA on CF are different to that one previously described. While the C=O band is preserved at 1720 cm^{-1} , even if its intensity decreases, new bands appear at close but slightly lower wavenumbers. Among them, the highest intensity band is centred around 1675 cm^{-1} . This could be assigned either to conjugated carbonyl compounds, such as conjugated aldehydes, ketones and acids, or to the stretching of carbon-carbon double bonds. Furthermore, one of these assignments or both of them are confirmed by the appearance of a high-intensity double band at 960 to 989 cm^{-1} , associated to C=C bending. In addition, the CH band almost disappeared. Once again, when the plasma-polymer is coated on the CF surface, evidence of appearance of new bands is given, bands characteristic of the formation of interfacial bonding between deposit and CF interface.

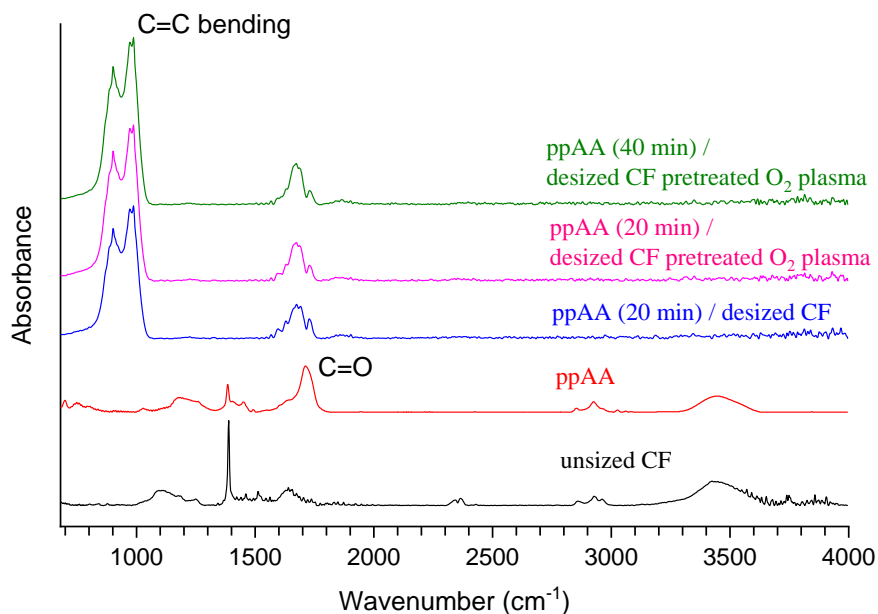


Fig. 5. Influence of the CF preparation (with or without O₂ plasma pre-treatment), of the duration of AA plasma-deposition (plasma parameters: p = 2 Pa, P = 10 W, DC = 8 %, v = 5kHz).

Table 5. Main FTIR bands assignment of the AA plasma-polymer

Wavenumber (cm ⁻¹)	Assignment
ppAA on KBr	
1383	CH ₃ bending
1720	C=O
2700 - 3000	C-H stretching
3400	OH
ppAA on CF	
960 - 989	C=C bending

Finally, O₂ pre-treatment and deposition duration did not induce a modification of the FTIR spectra. As performed before with ppHMDSO, SEM micrographs (Fig. 6) of the ppAA-CFs surface showed similar topography with a smooth layer covering of all surface cavities.

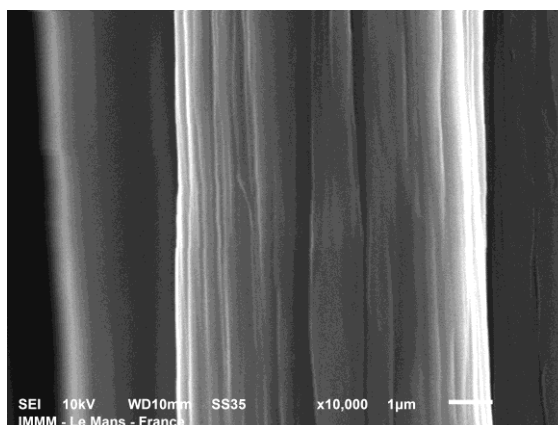


Fig. 6. SEM pictures (x10,000, 1 μm scale) of ppAA plasma-sized CF (plasma deposition: $p = 2 \text{ Pa}$, $P = 10 \text{ W}$, $\text{DC} = 8 \%$, $\nu = 5\text{kHz}$).

Within the study of the maleic anhydride plasma-deposition, the FTIR analyse (Fig. 7, Table 6) is more complex since the monomer and polymer signatures present many characteristic vibration bands [46, 47]. These characteristic bands of the anhydride function in the monomeric molecule are the following: C-O 1050 and 1250 cm^{-1} , C=O (conjugated anhydride, symmetric stretching) at 1780 cm^{-1} and the corresponding antisymmetric vibration mode at 1860 cm^{-1} , C=C bond stretching near 1600-1680 cm^{-1} . Nevertheless, the reactive anhydride can be hydrolysed and consequently in addition of -OH stretching at 3500 to 4000 cm^{-1} , a broad and intense band below 1780 cm^{-1} attributed to several carbonyl groups (aldehydes, ketones and carboxylic acids) appears. The ppMA coated on KBr pellet shows spectrum close to that of pure MA powder (Fig. 7, Table 6) even if some characteristic bands disappeared, especially those with weak intensity. Since the MA deposition rate is quite low, around $1.4 \pm 0.2 \text{ nm}\cdot\text{min}^{-1}$, these missing bands could be not detectable. However, other significant bands are still observable: C-O between 1050 and 1250 cm^{-1} . As the C=C vibration mode at 3100 cm^{-1} is not detected, the signal between 1600 to 1700 cm^{-1} are attributed to C=O indicating that MA polymerisation occurs via the double bond scission. OH groups are also identified near 3500 cm^{-1} . When the ppMA is layered on CF, its low deposition rate induces a

weak FTIR signal compared to that of CF. Nevertheless, the anhydride function bands are noticed around 1100 cm^{-1} plus two others between 3570 and 3750 cm^{-1} , characteristic of the OH stretching observed for on MA precursor spectrum.

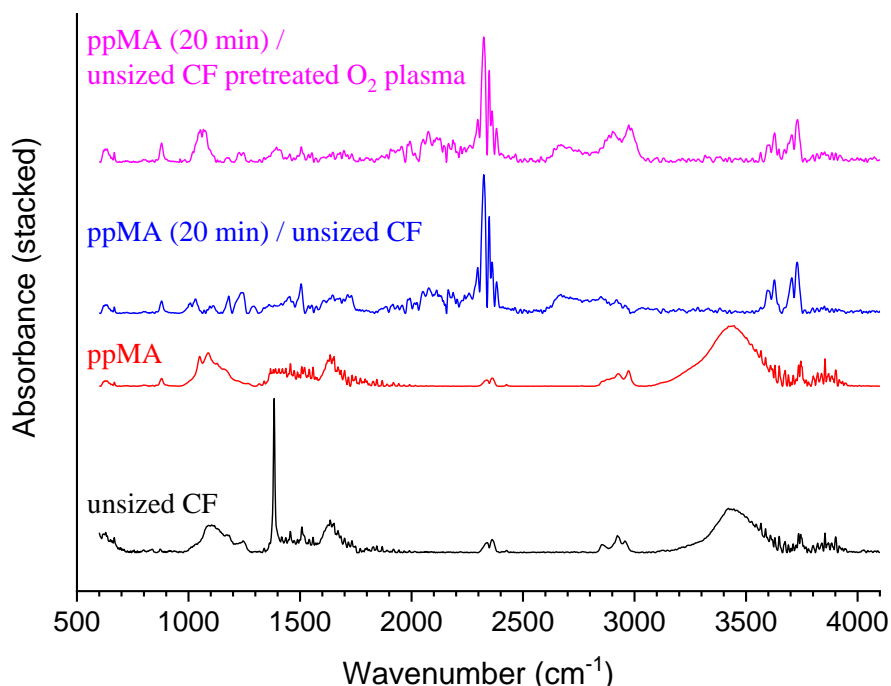


Fig. 7. Influence of the CF preparation (with or without O_2 plasma pre-treatment) (MA plasma parameters: $t = 20$ min, $p = 2$ Pa, $P = 10$ W, DC = 8 %, $\nu = 5\text{kHz}$).

Table 6. Main FTIR bands assignment of the MA plasma-polymer on KBr and CF

Wavenumber (cm^{-1})	Assignment
1050 and 1250	C-O
1600-1700	C=C or C=O
2150	CO_2
2900 to 3000	C-H (alkanes)
3500 - 4000	Internal and external OH bending

In an opposite manner to the study of ppHMDSO and ppAA layered on plasma-oxidized CF, such a pre-treatment of the CF improves the FTIR signal, as it is more pronounced, comprising stronger vibration modes of mainly aliphatic groups (C-H stretching) peaks.

Because leading to surface polarity and in some cases roughness, dioxygen plasma pre-treatment should enhance the adhesion of the precursor fragments and the ppMA itself on the CF, decreasing any subsequent deterioration of the thin film, showing a higher FTIR signal. Furthermore, with O₂ plasma pre-treatment, no new FTIR band is detected when the precursor is deposited on the CF, besides C-O bonds peaks (1050 to 1250 cm⁻¹) which appear stronger. This could indicate that this peak is partially significant of the appearance of new interfacial bonds (as C-O covalent bonds). Without the CF pre-oxidation, no difference is noticed meaning a weaker cohesion of the ppMA / CF assembly and therefore requiring the O₂ plasma pre-treatment.

As seen before with ppHMDSO (Fig. 4) and ppAA (Fig. 6), the ppMA-CF surface (Fig. 8) showed similar topography with no obvious change in the surface morphology of the CF, still suggesting local homogeneity of the deposition process.

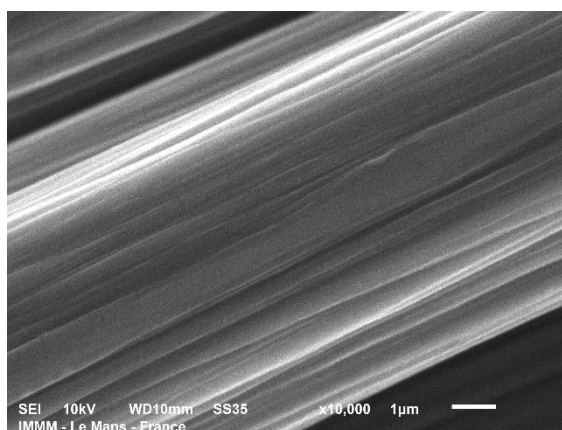


Fig. 8. SEM pictures (x10,000, 1µm scale) of ppMA plasma-sized CF (plasma deposition: p = 2 Pa, P = 10 W, DC = 8 %, v = 5kHz).

Finally, ppAc was also characterized in a same way as for the previous plasma-polymers. It should be noted, however, that this plasma-polymer cannot be directly compared with the previous ones since the plasma conditions are more drastic conditions in order to grow thicker films, but still with some retention degree of the functionality. FTIR spectra of ppAc (Fig. 9, Table 7) show several FTIR characteristic peaks such as C-H bending and CH stretching

bands at respectively 1380 cm^{-1} and $2900 - 3000\text{ cm}^{-1}$, whatever the deposition conditions. CH vibration indicates that saturated aliphatic compounds exist in the films. However, unsaturated groups are also identified with a small peak at 3100 cm^{-1} , corresponding to -CH (alkenes) stretching, leading to the conclusion of acetylene triple bond scission. Such molecular fragments lay on the surface as a plasma-polymer rich in carbon single and double bonds, confirmed by the presence of the characteristic band of the C=C bond stretching at 1610 cm^{-1} . The intensity of this latter band depends on the plasma parameters: the highest in relatively mild conditions (20 W, pulsed plasma) and decreasing with more drastic conditions (discharge power increasing from 20 to 40 W, plasma shifted to continuous mode). In these drastic plasma parameters, the triple bond of the acetylene molecule undergoes further chemical alteration and C=C proportion decreases in favour of saturated carbons, while oxidation takes place, mainly as carbonyl compounds (appearance of the characteristic band around 1700 cm^{-1}). With the pulsed mode, the oxidation is also noticed but at a lower degree mainly as C-O type compounds whose significant band is located at 1123 cm^{-1} .

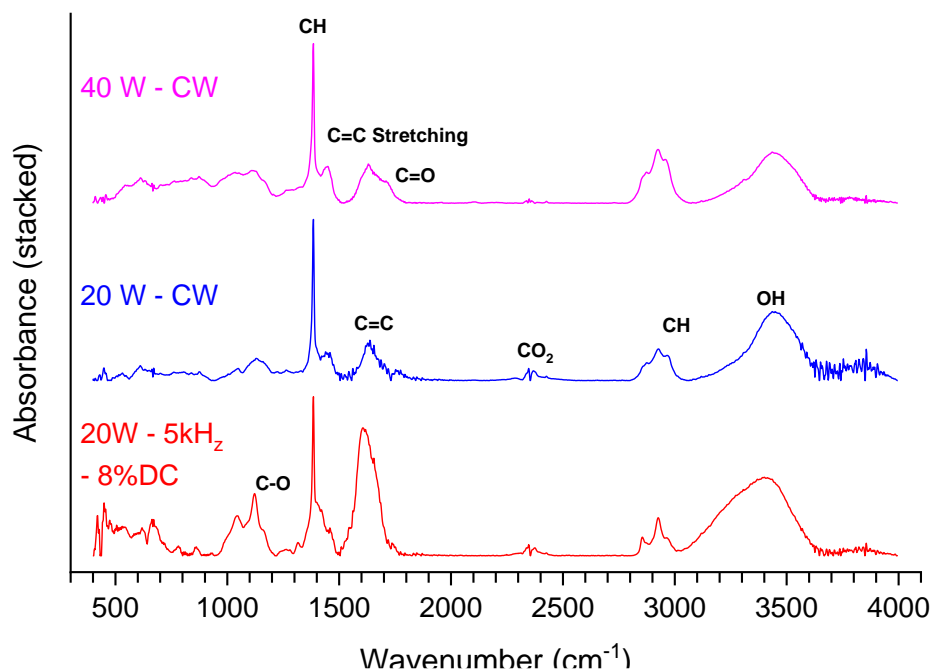


Fig. 9. Influence of the Ac plasma deposition (continuous or pulsed mode, discharge power) on the chemical composition of plasma-sized CF (plasma parameters: $p = 2$ Pa, $t = 40$ min).

Table 7. Main FTIR bands assignment of the Ac plasma-polymer.

Wavenumber (cm ⁻¹)	Assignment
ppAc on KBr	
1380	C-H bending
1123	C-O
1610	C=C
1700	C=O
2150	CO ₂
2900 to 3000	C-H (alkanes)
3000 to 3100	C-H (alkenes)
3500	OH bending

It should be noted that SEM micrographs of the ppAc thin films on CF (not shown here) gave similar type of pictures as for the previous deposits, i.e. the thin films did not change the aspect of the plasma-treated CF surface, which indicates once again local homogeneity of the deposition with filling of the initial cavities by the plasma polymer.

3.3 Dependence of the wettability of the plasma-modified carbon fiber on the plasma parameters

As stated previously, sizing allows to protect the CF integrity and provides potentially higher compatibility with the polymer matrix thanks to the thin film properties.[2, 4, 5] Chain interdiffusion [28], as well as surface physico-chemistry are important to ensure CF cohesion in the composites [34]. In the case of epoxy resins and some common polymer matrixes, acidic [32, 33] and polar surfaces are required [18-20]. In order to predict the sized-CF compatibility with any polymer matrix, quantification of the polarity of the surface is important as polar and acidic functions contribute to the surface polarity. The following study shows to what extent the different plasma-polymers studied here improve the surface wettability, as measured by quantifying the SFE, and especially the polar component.

Thus, several plasma conditions were studied for all of the previous organic precursors (Table 8). The mechanism of the plasma polymerization is controlled by the electronic impact on the precursor molecule and the followed monomer fragmentation and recombination leading to a large variety of surface chemical composition. The density of injected electron and precursors depend on the physical parameters such as discharge power, frequency of the pulses, gas flow rate and pressure. In order to preserve the precursor functionality, the plasma parameters as discharge power, duty cycle and impulse frequency were kept and varied as low as possible to sustain the plasma phase. Duration was fixed at 40 min in order to obtain a fairly thick deposit.

Table 8. Experimental conditions of the plasma-sizing of CF with ppHMDSO, ppAA, ppMA and ppAc

Precursor	Sample	P (W)	ν (kHz)	DC (%)	t (min)
HMDSO	HDMSO 1	10	5	8	40 min
	HDMSO 2	20	20	32	
	HDMSO 3	30	30	47	
MA	MA 1	10	5	8	
	MA 2	20	20	32	
	MA 3	30	30	47	
AA	AA 1	10	5	8	

	AA 2	10	10	16	
	AA 3	20	5	8	
	AA 4	20	20	32	
	AA 5	30	30	47	
Ac	Ac 1	40	continuous mode		60 min
	Ac 2	20			
	Ac 3	20	5	8	

Excepted ppAA / CF n° 2, 4 and 5 (Fig. 10), the surface free energy (SFE) of most of the plasma-polymers are similar and around value of 22 mJ/m², lower than the untreated fibre one's (27 ± 4 mJ/m²) with the respective dispersive and polar components at 17 ± 3 mJ/m² and 10 ± 4 mJ/m². More specifically, the dispersive component of the SFE slightly decreases from 17 ± 3 mJ/m² (untreated) to values around 15 mJ/m², with less discrimination between all of the samples. The polar component of the SFE shows however higher variations in its values, as it decreases from 11 ± 3 mJ/m² to values as low as 7 ± 3 mJ/m² (sample MA 1). Only 3 samples show slight improvement of the SFE: AA 2, AA 4 and AA 5, for which γ is measured as 29 ± 2 mJ/m² for AA 2 and AA 5, and 27 ± 3 mJ/m² for AA 4. Except for ppHMDSO, these values can be surprising as such polar and oxygen-rich monomers usually allow to attain very high SFE in the order of 70 mJ/m² with corresponding polar component of 50 mJ/m² (considering that the water contact angles near 0°), in the case of pp on planar surfaces, and confirmed in previous works [31, 45]. Indeed, above FTIR spectra of the different plasma-polymers showed significant traces of oxidation of the thin films. Even if their associated FTIR signal is a mean value on the overall thickness of deposit layer, evidence of surface oxidation should be detected by SFE measure. Such a discrepancy between apparent surface chemistry and measured SFE could be explained by the relatively low thickness of the thin films that could also be inhomogeneous over the total longer length, which was highlighted in the case of the ppMA study. As a matter of fact, ppHMDSO and ppAA had similar deposition rates, with film thickness (measured for planar surfaces of silicon wafers) respectively 120 ± 5 nm and 121 ± 15 nm at $P = 10$ W, $\nu = 5$ kHz, $DC = 8$ % and $t = 40$ min; ppMA showed the lowest deposition

rate of only few $\text{nm}\cdot\text{min}^{-1}$ ($1.4 \text{ nm}\cdot\text{min}^{-1}$ in these conditions) and thinner film equal to 52 ± 3 nm. Another explanation that cannot be excluded since the fiber is composed of 12000 strands deals with a shadow effect impeding the homogeneous deposition on each single strand. These variations in thickness or topography could induce a more complex wetting process as for an heterogeneous surface [48], thus lowering the effective surface free energies.

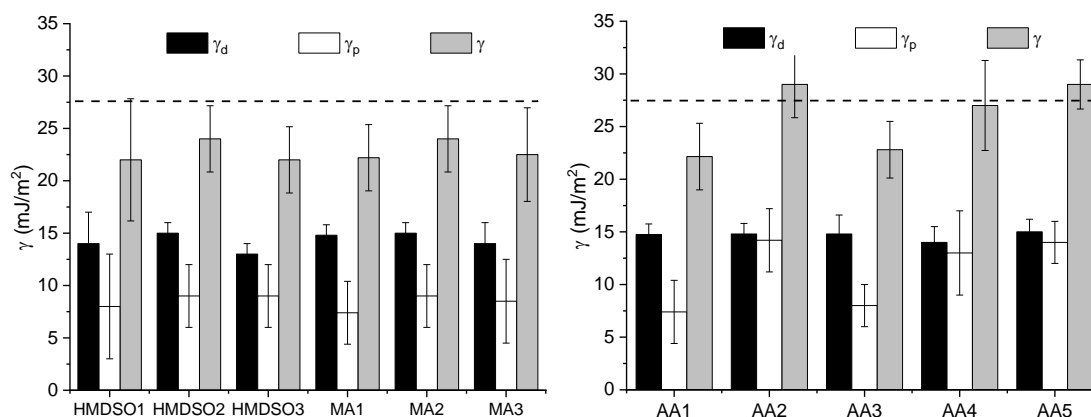


Fig. 10. Influence of the plasma conditions on surface free energy of the plasma polymers (HMDSO, MA and AA) deposited on the CF. The dashed line represents the surface free energy of the desized CF.

So, following this assumption, a thicker plasma-deposit, even if less functionalized should have more influence on the surface properties [15, 16]. Therefore, acetylene was chosen as another precursor as its deposition rate is usually very high compared to other organic precursor (several hundreds to thousands of $\text{nm}\cdot\text{min}^{-1}$ vs tens of $\text{nm}\cdot\text{min}^{-1}$ [49-51]) and will lead to a more hydrophobic, oleophobic surface.

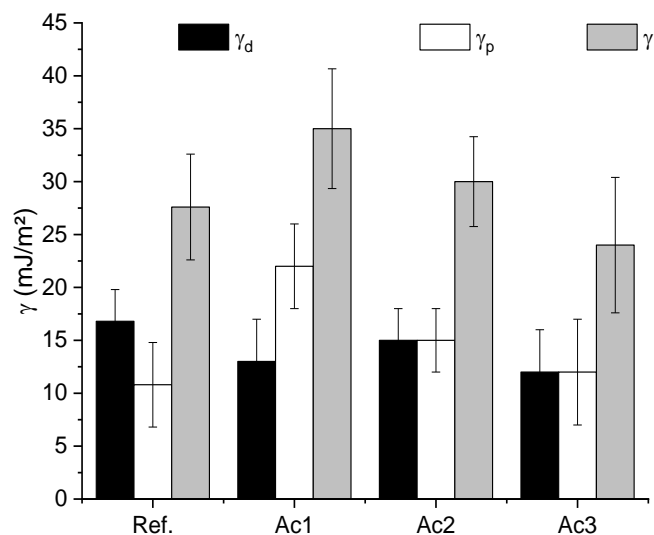


Fig. 11. Influence of the plasma conditions on surface free energy of thick ppAc deposited on the CF. Ref correspond to the surface free energy of the desized CF.

PpAc was deposited in more drastic conditions and specifically in continuous mode in order to enhance the monomer fragmentation and recombination. In such conditions, the obtained thickness for deposition on plane substrate is > 500 nm and its surface functionality is discussed in the previous chapter. Its surface free energy increases when the plasma conditions are stronger from 24 ± 6 to 30 ± 4 mJ/m² when the mode is shifted from pulsed to continuous and further increases up to 35 ± 5 mJ/m² when the power is doubled (Fig. 11). As seen here, the dispersive component of the surface free energy slightly decreases from 17 ± 3 (desized CF) to values around 12 ± 4 mJ/m². This decrease is low, regarding the dispersion of the values; the increase in the total SFE value observed is thus more likely dependent on the polar component, which is around the same value as the untreated CF (12 ± 5 vs 11 ± 4 mJ/m²) for the sample ppAc3 and increases up to 22 ± 4 mJ/m². This increase is explained by the thin film chemistry obtained from the FTIR measurements (Fig. 9). In pulsed conditions, high concentration of C=C bonds would impede the polarity of the surface, even if traces of C-O are detected. In continuous mode, the thin film is thicker, and loses a high proportion of carbon double bonds which can be extrapolated to the surface chemistry. The polarity increases thanks to lower

aliphatic carbons concentration while oxidized functions remain. With higher power, thickness increases again, C=C concentration is still low, and oxidation processes are more efficient, producing C=O functions, which contribute more to the surface polarity.

While significant polar group concentration is achieved with the deposition of acetylene, the surface chemistry, and especially the polarity, of ppAc are still of lower level than those obtained for the other plasma polymers (ppHMDSO, and especially ppAA and ppMA). Yet, ppAc gives better results for pp deposited on CF, and furthermore if surface oxidation is present. The main difference between ppAc and the other pp studied here is the higher deposition rate. Such experiment could indicate that the thickness of the deposited layer is prevalent on the surface polarity to improve the surface physico-chemistry of the CF. Thicker and more homogeneous along the fibre, the ppAc deposited onto CFs are more wetted than the pristine fiber are. Then, when the thickness of the layer is sufficient, the polarity of the thin film becomes prevalent.

Composites preparation requires a polymer matrix which is in most cases epoxy resin, a hydrophobic material; as carbon fiber are also hydrophobic, in order to obtain a cohesive composite, the matrix / fibre interface is reinforced thanks the chemical bond between these two elements. Therefore, more hydrophilic and compatible CF were prepared through two-step deposition (ppAc then ppMA) or codeposition of Ac and MA. As stated before, MA was chosen because it can promote CF adhesion in most of the polymer matrix thanks to its high polarity and reactivity.

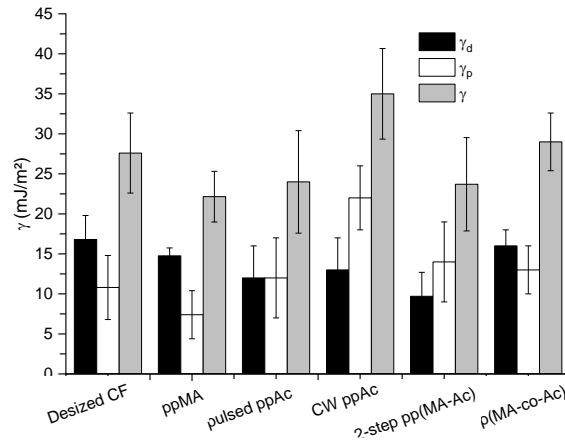


Fig. 12. Influence of the plasma conditions on surface free energy of different plasma polymer deposited on the CF (ppMA, ppAc -pulsed and CW), two-step ppMA-Ac, ppMA-co-Ac. Ref correspond to the surface free energy of the desized CF.

Fig. 12 shows the variation of the SFE for different plasma polymers deposited on CF. The ppMA-Ac sample refers to the ppAc deposited on the CF for 30 min in CW mode, followed by the deposition of ppMA for 30 min in same conditions as described before (10 W, 5 kHz, 8 %DC). The ppMA-co-Ac sample refers to the copolymer deposited for 30 min, for which the plasma polymerization occurred in a 50-50 % mixture of MA and C₂H₂ ($P = 10$ W, $\nu = 5$ kHz, $DC = 8$ %). The copolymer was also deposited on a ppAC (CW 30, min). From Fig. 10, the deposition of a bilayer ppMA-Ac does not improve the wettability of the CF surface in comparison with the sole ppMA which respective SFE values are 22 ± 3 and 23 ± 4 mJ/m². On the other hand, the copolymer shows intermediate wettability as the SFE value (29 ± 3 mJ/m²) is comprised between that one pulsed ppAC ($\gamma = 24 \pm 6$ mJ/m²) and CW-ppAc one $\gamma = 35 \pm 5$ mJ/m². It appears that the growth of a polar thin layer over a thick plasma polymer layer does not improve the wettability. In fact, such observation is explained by the fact that whatever lies beneath the ppMA, i.e. either the pristine CF or a ppAc-sized CF, the wetting behaviour is the same: the ppAc first layer does not prevent or counter the potential inhomogeneities of the ppMA thin film. Then, the better wettability obtained for the copolymer, in comparison with ppAc in pulsed conditions, could be explained here by a difference in the surface chemistry.

Indeed, the codeposition of MA with Ac induces less inhomogeneities as it benefits from the higher deposition rate of acetylene, while promoting the surface chemistry thanks to MA. The copolymer presents more polar groups thanks to the MA monomer than the ppAc which showed high concentration of carbon double bands. Yet, high concentration of carbon double bonds (highlighted in these plasma conditions in Fig. 9) compete with the MA functionality and reduce the maximal polarity attainable by the pp surface. The copolymer is then less efficient than ppAc deposited at 40 W (continuous mode) as seen in Fig. 12, which seems to be polar thanks to significant concentration of C=O type groups, and benefiting from even higher thickness thanks to the deposition parameters and the intrinsic high deposition rate of acetylene. Nevertheless, this study shows that the combination of high concentration of polar groups on the surface with homogeneous distribution, with the large and homogeneous thickness of the thin films is needed to efficiently improve the CF surface properties. A possible way of improvement would be to grow a thick layer of ppAc, followed by a concentration-gradient pp(MA-co-Ac): during deposition, decreasing the Ac proportion while maintaining a total flow rate constant. This would reduce surface inhomogeneities, while ensuring high polarity of the surface as the extreme surface layer would be mostly comprised of ppMA.

4. Conclusion

This study showed that RF plasma polymerization of HMDSO, AA and MA is quite efficient to grow plasma polymer thin films on the CF surface. FTIR analysis of the sole thin films in comparison with the analysis of the thin films deposited on CF, highlighted formation of new bonds, which indicates formation of covalent bonds at the plasma polymer – CF

interface. Such bonds could improve the cohesion of the thin films and thus the mechanical properties of the composite formed with such surface-treated CF.

Wettability measurements showed however that most of the plasma polymers considered did not improve the physicochemical properties of the CF surfaces. Indeed, plasma polymers grown in drastic conditions showed better results of surface wetting, in spite of the fact that such deposition conditions should induce a loss of the precursor functionality in the polymer thin film. The plasma polymerization of acetylene in drastic conditions indeed showed the highest wettability increase of the CF treated surfaces. This observation was assigned to the high deposition rate of ppAc, which allows to grow more homogeneous plasma polymers on the CF, mainly in terms of thickness. This means that low thickness thin film induces partial wetting as the coverage of the CF is not total. However, when the thickness of the thin film is sufficient, the surface chemistry has to be taken into account. Indeed, in conditions that allowed the ppAc to oxidize its surface (as seen by FTIR measurements by the presence of oxygenated functions such as C-O and C=O), or by growing a copolymer with a polar precursor, the wettability of the CF was further increased, up to the doubling of the SFE value of the pristine CF.

Acknowledgments

This study is part of the FORCE project supported by IRT Jules Verne (French Institute in Research and Technology in Advanced Manufacturing Technologies for Composite, Metallic and Hybrid Structures). The authors wish to associate the industrial and academic partners of this project; respectively Faurecia, Arkema, Mersen, PSA, Renault, Décathlon, DGA, CEA, Chantiers de l'Atlantique, CANOE.

4. References

- [1] J.-K. Kim, Y.W. Mai, *Engineered interfaces in fiber reinforced composites*, Elsevier Sciences, 1998.
- [2] S. Tiwari, J. Bijwe, *Surface Treatment of Carbon Fibers - A Review*, *Procedia Technol.* 14 (2014) 505–512. doi:10.1016/j.protcy.2014.08.064.
- [3] C. Cherif, *Textile Materials for Lightweight Constructions*, Springer Berlin Heidelberg, Berlin, Heidelberg, 2016. doi:10.1007/978-3-662-46341-3.
- [4] N. Raphael, K. Namratha, B.N. Chandrashekar, K.K. Sadasivuni, D. Ponnamma, A.S. Smitha, S. Krishnaveni, C. Cheng, K. Byrappa, *Surface modification and grafting of carbon fibers: A route to better interface*, *Prog. Cryst. Growth Charact. Mater.* 64 (2018) 75–101. doi:10.1016/j.pcrysgrow.2018.07.001.
- [5] M. Sharma, S. Gao, E. Mäder, H. Sharma, L.Y. Wei, J. Bijwe, *Carbon fiber surfaces and composite interphases*, *Compos. Sci. Technol.* 102 (2014) 35–50. doi:10.1016/j.compscitech.2014.07.005.
- [6] A. Kafi, M. Huson, C. Creighton, J. Khoo, L. Mazzola, T. Gengenbach, F. Jones, B. Fox, *Effect of surface functionality of PAN-based carbon fiber on the mechanical performance of carbon/epoxy composites*, *Compos. Sci. Technol.* 94 (2014) 89–95. doi:10.1016/j.compscitech.2014.01.011.
- [7] R.L. Zhang, Y.D. Huang, L. Liu, Y.R. Tang, D. Su, L.W. Xu, *Effect of emulsifier content of sizing agent on the surface of carbon fiber and interface of its composites*, *Appl. Surf. Sci.* 257 (2011) 3519–3523. doi:10.1016/j.apsusc.2010.11.066.
- [8] J. Liu, H. Ge, J. Chen, D. Wang, H. Liu, *The preparation of emulsion type sizing agent for carbon fiber and the properties of carbon fiber/vinyl ester resin composites*, *J. Appl. Polym. Sci.* 124 (2012) 864–872. doi:10.1002/app.35126.
- [9] B. Yameen, M. Álvarez, O. Azzaroni, U. Jonas, W. Knoll, *Tailoring of Poly(ether ether ketone) Surface Properties via Surface-Initiated Atom Transfer Radical Polymerization*, *Langmuir.* 25 (2009) 6214–6220. doi:10.1021/la900010z.
- [10] D.S. Wavhal, E.R. Fisher, *Hydrophilic modification of polyethersulfone membranes by low temperature plasma-induced graft polymerization*, *J. Memb. Sci.* 209 (2002) 255–269. doi:10.1016/S0376-7388(02)00352-6.
- [11] W. Kowbel, C. Bruce, J.C. Withers, P.O. Ransone, *Effect of carbon fabric whiskerization on mechanical properties of C-C composites*, *Compos. Part A Appl. Sci. Manuf.* 28 (1997) 993–1000. doi:10.1016/S1359-835X(97)00007-9.
- [12] C. Fang, J. Wang, T. Zhang, *Interlaminar improvement of carbon fiber/epoxy composites via depositing mixture of carbon nanotubes and sizing agent*, *Appl. Surf. Sci.* 321 (2014) 1–9. doi:10.1016/j.apsusc.2014.09.170.
- [13] G. Le Dû, N. Celini, F. Bergaya, F. Poncin-Epaillard, *RF plasma-polymerization of acetylene: Correlation between plasma diagnostics and deposit characteristics*, *Surf. Coatings Technol.* 201 (2007) 5815–5821. doi:10.1016/j.surfcoat.2006.10.025.
- [14] D. Debarnot, T. Mérian, F. Poncin-Epaillard, *Film Chemistry Control and Growth Kinetics of Pulsed Plasma-Polymerized Aniline*, *Plasma Chem. Plasma Process.* 31 (2011) 217–231. doi:10.1007/s11090-010-9271-2.
- [15] N. Dilsiz, E. Ebert, W. Weisweiler, G. Akovali, *Effect of Plasma Polymerization on Carbon Fibers Used for Fiber/Epoxy Composites*, *J. Colloid Interface Sci.* 170 (1995) 241–248. doi:10.1006/jcis.1995.1093.
- [16] Z.-F. Li, A.N. Netravali, *Surface modification of UHSPE fibers through allylamine plasma deposition. II. Effect on fiber and fiber/epoxy interface*, *J. Appl. Polym. Sci.* 44 (1992) 333–346. doi:10.1002/app.1992.070440217.

- [17] A.P. Kettle, F.R. Jones, M.R. Alexander, R.D. Short, M. Stollenwerk, J. Zabold, W. Michaeli, W. Wu, E. Jacobs, I. Verpoest, Experimental evaluation of the interphase region in carbon fibre composites with plasma polymerised coatings, *Compos. Part A Appl. Sci. Manuf.* 29 (1998) 241–250. doi:10.1016/S1359-835X(97)00088-2.
- [18] C. Roux, J. Denault, M.F. Champagne, Parameters regulating interfacial and mechanical properties of short glass fiber reinforced polypropylene, *J. Appl. Polym. Sci.* 78 (2000) 2047–2060. doi:10.1002/1097-4628(20001213)78:12<2047::AID-APP10>3.0.CO;2-Z.
- [19] S.H. Han, H.J. Oh, S.S. Kim, Evaluation of fiber surface treatment on the interfacial behavior of carbon fiber-reinforced polypropylene composites, *Compos. Part B Eng.* 60 (2014) 98–105. doi:10.1016/j.compositesb.2013.12.069.
- [20] D.T. Burn, L.T. Harper, M. Johnson, N.A. Warrior, L. Yang, J. Thomason, The influence of coupling agent, fibre sizing and matrix degradation on the interfacial shear strength between carbon fibre and polypropylene, 16th Eur. Conf. Compos. Mater. ECCM 2014. (2014) 22–26.
- [21] G. Dagli, N.-H. Sung, Properties of carbon/graphite fibers modified by plasma polymerization, *Polym. Compos.* 10 (1989) 109–116. doi:10.1002/pc.750100208.
- [22] D.A. Biro, G. Pleizier, Y. Deslandes, Application of the microbond technique. IV. Improved fiber–matrix adhesion by RF plasma treatment of organic fibers, *J. Appl. Polym. Sci.* 47 (1993) 883–894. doi:10.1002/app.1993.070470516.
- [23] J.B. Donnet, G. Guilpain, Surface characterization of carbon fiber, *Composites.* 22 (1991) 59–62. doi:10.1016/0010-4361(91)90104-O.
- [24] D.K. Owens, R.C. Wendt, Estimation of the surface free energy of polymers, *J. Appl. Polym. Sci.* 13 (1969) 1741–1747. doi:10.1002/app.1969.070130815.
- [25] D.G.A.L. Aarts, J.H. Van Der Wiel, H.N.W. Lekkerkerker, Interfacial dynamics and the static profile near a single wall in a model colloid-polymer mixture, *J. Phys. Condens. Matter.* 15 (2003). doi:10.1088/0953-8984/15/1/332.
- [26] A. Manakhov, M. Michlíček, D. Nečas, J. Polčák, E. Makhneva, M. Eliáš, L. Zajíčková, Carboxyl-rich coatings deposited by atmospheric plasma co-polymerization of maleic anhydride and acetylene, *Surf. Coatings Technol.* 295 (2016) 37–45. doi:10.1016/j.surfcoat.2015.11.039.
- [27] W. Weisweiler, K. Schlitter, Surface modification of carbon fiber by plasma polymerization, *Thin Solid Films.* 207 (1992) 158–165. doi:10.1016/0040-6090(92)90117-T.
- [28] S.S. Voyutskii, V.L. Vakula, The role of diffusion phenomena in polymer-to-polymer adhesion, *J. Appl. Polym. Sci.* 7 (1963) 475–491. doi:10.1002/app.1963.070070207.
- [29] M. Endou, S. Ueno, T. Hongu, M. Takamizawa, Carbon fibers having improved surface properties and a method for the preparation thereof, US Patent 4,596,741, 1986.
- [30] A.P. Kettle, A.J. Beck, L. O’Toole, F.R. Jones, R.D. Short, Plasma polymerisation for molecular engineering of carbon-fibre surfaces for optimised composites, *Compos. Sci. Technol.* 57 (1997) 1023–1032. doi:10.1016/S0266-3538(96)00162-5.
- [31] T.H. Tran, D.B. Au, B. Diawara, K. Fatyeyeva, S. Marais, J. Ortiz, D. Debarnot, F. Poncin-Epaillard, How the chemical structure of the plasma-deposited SiO_x film modifies its stability and barrier properties: FTIR study, *Prog. Org. Coatings.* (2019). doi:10.1016/j.porgcoat.2019.105332.
- [32] Z. Dai, B. Zhang, F. Shi, M. Li, Z. Zhang, Y. Gu, Chemical interaction between carbon fibers and surface sizing, *J. Appl. Polym. Sci.* 124 (2012) 2127–2132. doi:10.1002/app.35226.
- [33] N. Dilsiz, J. Wightman, Effect of acid–base properties of unsized and sized carbon fibers on fiber/epoxy matrix adhesion, *Colloids Surfaces A Physicochem. Eng. Asp.* 164 (2000)

- 325–336. doi:10.1016/S0927-7757(99)00400-8.
- [34] K. Horie, M. Hiromichi, I. Mita, Bonding of epoxy resin to graphite fiber, *Fibre Sci. Technol.* 9 (1976) 253–264. doi:10.1016/0015-0568(76)90008-7.
- [35] L. Altay, E. Bozaci, M. Atagur, K. Sever, G.S. Tantug, M. Sarikanat, Y. Seki, The effect of atmospheric plasma treatment of recycled carbon fiber at different plasma powers on recycled carbon fiber and its polypropylene composites, *J. Appl. Polym. Sci.* 136 (2019) 47131. doi:10.1002/app.47131.
- [36] A. Ferrari, J. Robertson, Interpretation of Raman spectra of disordered and amorphous carbon, *Phys. Rev. B - Condens. Matter Mater. Phys.* 61 (2000) 14095–14107. doi:10.1103/PhysRevB.61.14095.
- [37] S. Bernard, O. Beyssac, K. Benzerara, N. Findling, G. Tzvetkov, G.E. Brown, XANES, Raman and XRD study of anthracene-based cokes and saccharose-based chars submitted to high-temperature pyrolysis, *Carbon N. Y.* 48 (2010) 2506–2516. doi:10.1016/j.carbon.2010.03.024.
- [38] L. Bokobza, J.-L. Bruneel, M. Couzi, Raman spectroscopy as a tool for the analysis of carbon-based materials (highly oriented pyrolytic graphite, multilayer graphene and multiwall carbon nanotubes) and of some of their elastomeric composites, *Vib. Spectrosc.* 74 (2014) 57–63. doi:10.1016/j.vibspec.2014.07.009.
- [39] F. Vautard, S. Ozcan, F. Paulauskas, J.E. Spruiell, H. Meyer, M.J. Lance, Influence of the carbon fiber surface microstructure on the surface chemistry generated by a thermochemical surface treatment, *Appl. Surf. Sci.* 261 (2012) 473–480. doi:10.1016/j.apsusc.2012.08.038.
- [40] E. Frank, L.M. Stuedle, D. Ingildeev, J.M. Sporl, M.R. Buchmeiser, Carbon fibers: Precursor systems, processing, structure, and properties, *Angew. Chemie - Int. Ed.* 53 (2014) 5262–5298. doi:10.1002/anie.201306129.
- [41] O. Paris, C. Zollfrank, G.A. Zickler, Decomposition and carbonisation of wood biopolymers — a microstructural study of softwood pyrolysis, *Carbon N. Y.* 43 (2005) 53–66. doi:10.1016/j.carbon.2004.08.034.
- [42] M.R. Snowdon, A.K. Mohanty, M. Misra, A study of carbonized lignin as an alternative to carbon black, *ACS Sustain. Chem. Eng.* 2 (2014) 1257–1263. doi:10.1021/sc500086v.
- [43] N. Byrne, M. Setty, S. Blight, R. Tadros, Y. Ma, H. Sixta, M. Hummel, Cellulose-Derived Carbon Fibers Produced via a Continuous Carbonization Process : Investigating Precursor Choice and Carbonization Conditions, *Macromol. Chem. Phys.* 217 (2016) 2517–2524.
- [44] N. V. Chukanov, A.D. Chervonnyi, IR Spectra of Minerals and Related Compounds, and Reference Samples' Data, in: 2016: pp. 51–1047. doi:10.1007/978-3-319-25349-7_2.
- [45] T.H. Tran, D. Debarnot, J. Ortiz, F. Poncin-Epaillard, Plasma codeposition of transparent thin films: Relationship between the surface chemistry and the anti-fogging property, *Plasma Process. Polym.* 16 (2019) 6–10. doi:10.1002/ppap.201900070.
- [46] B.C. Smith, *Infrared spectral interpretation : a systematic approach*, CRC Press, 1999.
- [47] M.E. Ryan, A.M. Hynes, J.P.S. Badyal, Pulsed plasma polymerization of maleic anhydride, *Chem. Mater.* 8 (1996) 37–42. doi:10.1021/cm9503691.
- [48] A.B.D. Cassie, S. Baxter, Wettability of porous surfaces, *Trans. Faraday Soc.* 40 (1944) 546. doi:10.1039/tf94444000546.
- [49] H. Yasuda, T. Hirotsu, Polymerization of organic compounds in an electrodeless glow discharge. IX. Flow-rate dependence of properties of plasma polymers of acetylene and acrylonitrile, *J. Appl. Polym. Sci.* 21 (1977) 3167–3177. doi:10.1002/app.1977.070211127.
- [50] L. Zajíčková, S. Rudakowski, H.W. Becker, D. Meyer, M. Valtr, K. Wiesemann, Study

- of plasma polymerization from acetylene in pulsed r.f. discharges, *Thin Solid Films*. 425 (2003) 72–84. doi:10.1016/S0040-6090(02)01133-1.
- [51] N.I. Kim, H.M. Kang, Y.T. Hong, T.H. Yoon, Plasma etching and plasma polymerization coating of carbon fibers. Part 2. Characterization of plasma polymer coated carbon fibers, *J. Adhes. Sci. Technol.* 16 (2002) 1825–1838. doi:10.1163/156856102320396166.